4 Thin film synthesis

In the adsorption experiments with single crystals the observed effects are not strictly related to thermodynamic equilibrium, as only a near-surface area was intercalated. In order to force the deposited alkali to form homogenous phases TMDC thin films have been synthesized in UHV. TiS_2 has been chosen as material, due to the large number of investigations and calculations related to its alkali intercalation. After an introduction to the thin film synthesis techniques in UHV the electronic structure of TiX_2 will be shortly described before the effects of the different experimental parameters on the film properties will be presented.

4.1 Low-pressure growth techniques

The deposition of thin films at high- or ultra-high-vacuum conditions has emerged in the last two decades as the leading technology in preparing compound semiconductor heterostructures. This section summarizes the introduction given in a recent book [148] that reviews the technique and its progresses in the synthesis of several semiconductor systems. The deposition flux can be precisely controlled and it is possible to prepare very pure materials of monolayer thickness. Basically two techniques have been established, which differ in the nature of the sources used, and are schematically represented on top of Fig. 4.1. In molecular beam epitaxy (MBE) atomic (e.g. Al, Ga, In) or molecular (As_4, P_4, S_8) beams are generated in effusion cells typically by heating the solid elements. Very low pressures can be used (10^{-5} -10^{-9} mbar) due to the high sticking coefficient of the pure elements. Once adsorbed the atoms diffuse to the appropriate lattice sites, and may be deposited epitaxially. In chemical vapor deposition (CVD) volatile chemical compounds containing the needed elements to deposit are used. Typically liquid organometallic compounds are evaporated at room temperature; then the technique is called molecular organic CVD (MOCVD). In CVD pressures in the order of 1 mbar are used, and the molecules typically decompose already in the stagnant boundary layer above the heated substrate. Gas-phase reactions are also possible. If pressures lower than $5 \cdot 10^{-4}$ mbar are used, also with molecular sources a beam is generated, as the free mean path of the precursors is larger than the distance source-substrate. Therefore no stagnant gas layer covers the substrate, which is directly hit by the molecules. At its surface the molecule may soon desorb, or acquire thermal energy from the substrate and decompose, typically by cleaving the bonds between the needed element and its ligands or organic radicals. This third technique with its specific growth mechanism has been called chemical beam epitaxy (CBE) by Tsang in 1984 [149], who first could obtain device quality materials from gaseous sources only. Advantages of CBE vs. MBE include an easier control of the evaporation rate and a better lateral

uniformity, if the sources are premixed in one beam. Moreover flow patterns, as is typically found in MOCVD reactors are absent. As the sticking coefficient largely depends on the surface-catalyzed reaction, the growth is strongly influenced by the nature of the substrate. This kind of selectivity is lower in MBE, which has higher sticking coefficients, or in MOCVD, where decomposition reactions partly occurs in the more concentrated gas phase. For similar reasons the composition and growth rates obtained in CBE are more sensitive to the substrate temperature.

As low-pressure techniques are mainly of interest for electronic device quality materials, no MBE or CBE depositions are reported in the literature for semimetals like TiX_2. Only CVD growth has been reported for these materials [111, 150, 151].

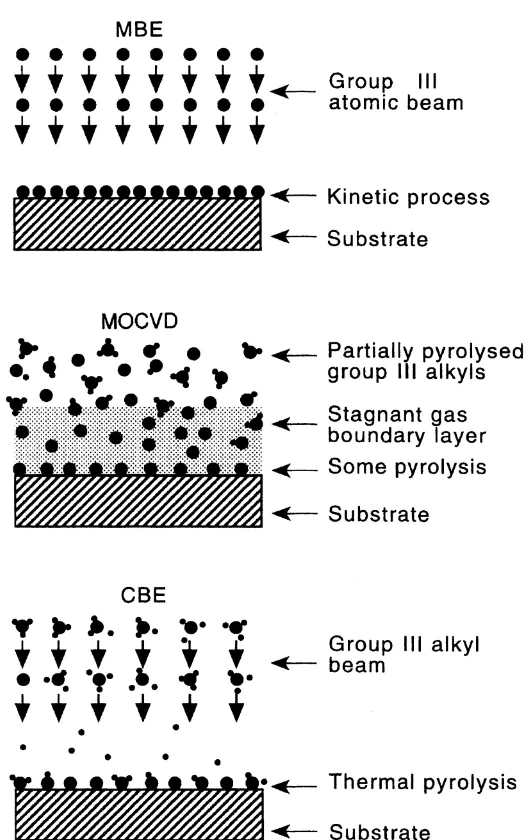

Fig. 4.1 Schematic representation of the growth processes involved in the main low-pressure deposition techniques. After ref. [148]

4.2 The electronic structure of TiX_2

The optimization of the preparation conditions of TiX_2 was based on the XPS/UPS characterization. An understanding of the electronic structure of the compounds to be prepared was necessary to properly guide the variation of parameters

Despite the large number of investigations it is a still open question whether 1T-TiS_2 is a small band gap semiconductor or a semimetal. Whereas it is well accepted that the Fermi level is situated between the conduction bands mainly derived of Ti 3d orbitals and the valence bands from S 3p orbitals, results do not agree with respect to the separation of the two bands. Earlier

calculations predict a gap between these bands [152-155]. Some experimental evidences support the existence of a small band gap. Pressure-dependent measurements of the transport properties [156], ARUPS [157], and STM [158] studies found a band gap of 0.1-0.5 eV. The fact that at best a stoichiometry of $Ti_{1.002\pm0.001}S_2$ was obtained [159] indicates that in most cases some excess Ti is always present. Ti in excess occupies sites in the van der Waals gap leading to a so-called self-intercalated compound. From a comparison of compositional analysis and transport measurements it can be shown that at least for low self-intercalation levels up to $Ti_{1.05}TiS_2$ four electrons per titanium atoms are transferred to the conduction band. Due to this large extrinsic doping levels the compound has been considered as a degenerated semiconductor with metallic conductivity [159]. However, other reports based on PES [160, 161] or electrical properties as function of stoichiometry [162] suggested a band gap of less than 0.1 eV or an overlap of S 3p and Ti 3d bands. Also some calculations indicate an overlap of bands [43, 163]. Recent *ab-initio* localized spherical wave calculations, which differentiated between the electronic structures of bulk TiS_2 and a slab of TiS_2, have shown that a slab is an intrinsic semiconductor, while bulk TiS_2 is a semimetal [40]. This may explain the results based on surface-sensitive techniques like electroreflectance and UPS, which tend to indicate semiconducting behavior. The semimetallic nature of TiS_2 is confirmed by full-potential calculations [45], which however indicate that also a single slab is semimetallic. These results contradict earlier Hartree-Fock calculations which have quoted that TiS_2 is a semiconductor for pressures below 4 GPa [44]. Although most modern calculations seem to indicate rather small band gaps or overlap between S and Ti bands, the tendency of the widely used local density approximation (LDA) to underestimate the band gap has been emphasized [47].

Calculations are more consistent for $TiSe_2$ reporting its semimetallic properties [40].

The DOS at the band gap of $Ti_{1+x}S_2$ for different stoichiometries has been measured with STS (scanning tunneling spectroscopy) in ref. [158]. An empirical formula relating the position of the Fermi level to the amount of excess Ti was given:

$$E_{CB} - E_F = -0.67 - 0.24\ln(x + 0.02) \quad \textit{(Eq. 4.1).}$$

Given the filling of the conduction band, E_F (the PES reference level) shifts to higher energy with increasing x. Consequently the substrate levels for higher x should tend to higher BE. This effect is expected to be most important only for the chalcogen signals. The charge transferred to Ti 3d states partly screens the Ti core levels, and no net shift is observed. Following the occupation of the Ti 3d electrons also a lifetime broadening is induced to the 2p core-hole through a super-Coster-Kronig Auger transition [164]. As a consequence all peaks exhibit an enhanced asymmetry, which is directly induced by the higher density of states at E_F [165, 166].

4.3 Optimization

Besides the complexity of the CBE process the preparation of sulfides is in general difficult. Sulfides usually form many different phases, dependent on their defect structure. In Fig. 4.2 it can be seen that the phase diagram for the S-Ti system is no exception, and the author warns that this is only a tentative diagram [167]. Nineteen distinct structures are observed in the range between TiS and TiS_2 corresponding to different occupancy of Ti atoms in the vdW gap. CBE growth conditions do not correspond to a thermodynamic equilibrium state, and the growth situation is tremendously complicated not only due to use of precursors different from the simple elements, but also due to the kinetic processes involved. Therefore the optimization of the preparation conditions remains an empirical process, whose parameters depend also on the reactor geometry. The optimization is necessary even in the case when a preparation is already reported in the literature.

The formation of stoichiometric TiS_2 is particularly important for the intercalation reaction. Any excess Ti residing in the vdW gap pins the host layers together, slowing down or even preventing intercalation [168].

Below the parameters are reported, which have been varied in order to obtain suitable TiS_2 thin films. A roughly chronological order during the optimization process is followed.

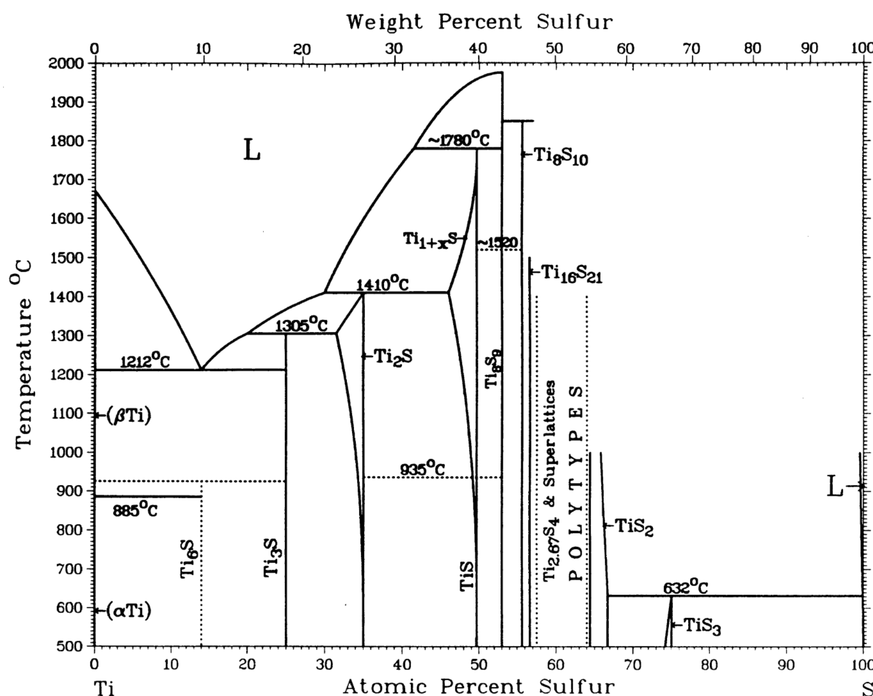

Fig. 4.2 Phase diagram for the S-Ti system. After ref. [167]

4.3.1 Precursors

The growth was performed in an UHV chamber with base pressure of $<10^{-8}$ mbar. Substrates of different surface properties and at a controlled temperature were exposed to the simultaneous flux of Ti and S precursors for times ranging from a few minutes to several hours.

S sources

H_2S and hexamethyldisilylthiane (HMDST formula $(H_3C)_3Si\text{-}S\text{-}Si(CH_3)_3$) are widely used S sources in wet chemical [169-173], as well as in vapor phase synthesis [150, 174-184] of layered sulfides. Especially the Si-S bond in HMDST was expected to be very reactive. But using these precursors it was not possible to obtain any significant sulfide deposition at pressures below 10^{-4} mbar using different substrates, Ti compounds and temperatures. It can be noted that both these molecules contain a singular S as bridging heteroatom.

However, using S_2 (evaporated from heating FeS_2) and tertbutyldisulfide (TBDS, $(H_3C)_3C\text{-}S\text{-}S\text{-}C(CH_3)_3$), sulfidation and/or deposition could easily be obtained. TBDS has already successfully been used in MOCVD synthesis of pyrite thin films [185-189]. FeS_2 heated in a crucible produces S_2, which promptly reacts with transition metals. Similar results were obtained with TBDS suggesting analogous reaction paths that are distinct from the monosulfide species. TBDS is a liquid under standard conditions. Thus the evaporation rate can easily be controlled by regulating the inlet valve to obtain the chosen stationary partial pressure. By decomposing pyrite instead the only control is by the crucible temperature. The S_2 yield is expected to slowly decrease with time. The measurement of the S_2 partial pressure by mean of a mass spectrometer cannot be used for flux control routinely given the high reactivity of this species.

Ti sources

Ti was obtained either by direct evaporation from a metallic wire or from $TiCl_4$. Despite Ti is tetravalent in $TiCl_4$ as well as in TiS_2 if the substrate temperature was high or the S flux small the binding energy of the Ti 2p line was close to that of metallic Ti (Fig. 4.1). Using a metallic wire larger amounts of not fully reacted Ti were found. At lower temperature no large Ti excess can be obtained, being $TiCl_4$ stable to the thermal decomposition (see §4.4). The CBE source was also preferred here to ensure a more reliable control of the flux rate.

4.3.2 Substrate

The problem of precursor adsorption on the substrate is crucial at low pressures as is clearly shown by the variation of the substrate. Metallic (Mo, stainless steel, Ta, Ti, Au) and ceramic (SiO_2, Al_2O_3) substrates have been tested at temperatures ranging from 150°C to 700°C. A significant deposition was observed on ceramic substrates only if an excess of metallic Ti was previously deposited from a filament.

On Mo foil the dominant reaction was the substrate sulfidation. The Mo 3d doublet shows two components demonstrating a surface reaction (Fig. 4.4). The S 2p signal indicates the formation of a sulfide, but only small Ti amounts were found. No thick layer of Ti sulfide could be observed.

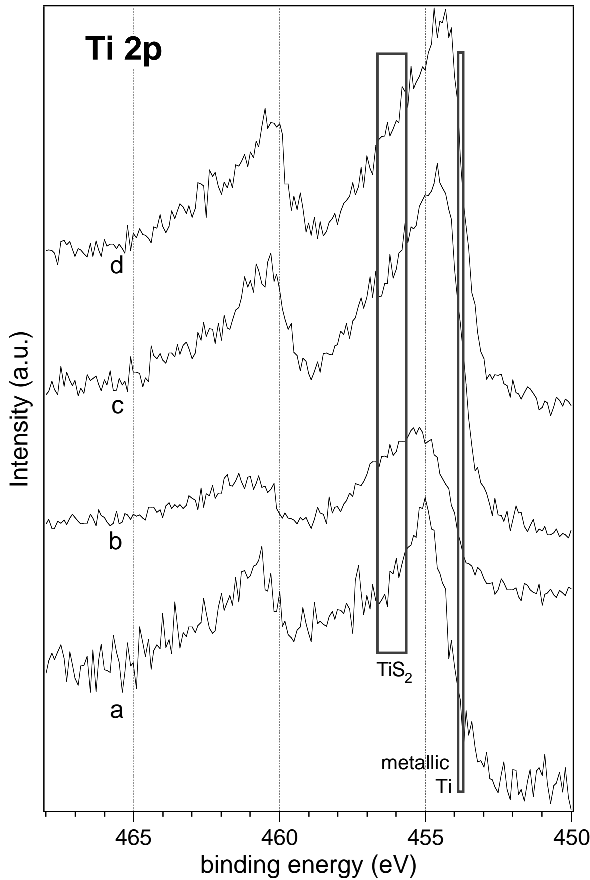

Fig. 4.3 Ti 2p core-level signal for thin films deposited with S_2 on stainless steel for 30 min. Meanings of the letters are summarized in the table below

sample	***Ti source***	***S source T***	***Substr.T***
d	*Ti 44 A*	*265°C*	*450°C*
c	*$TiCl_4$ 10^{-5} mbar*	*265°C*	*450°C*
b	*$TiCl_4$ 10^{-5} mbar*	*280°C*	*450°C*
a	*$TiCl_4$ 10^{-5} mbar*	*off*	*510°C*

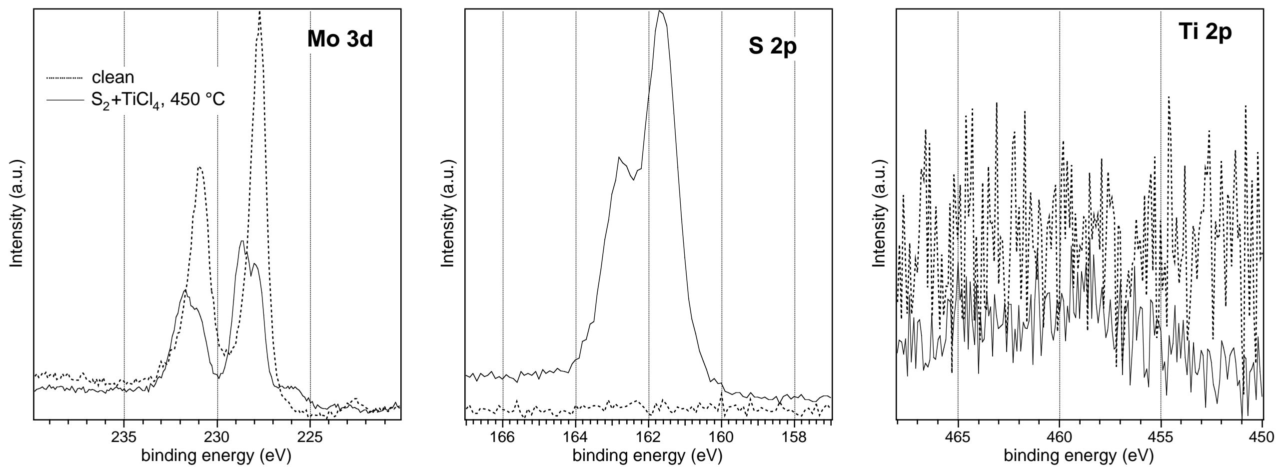

Fig. 4.4 Core-level signals of substrate and deposited elements after 30 min deposition of S_2 and $TiCl_4$ (10^{-4} mbar) on a hot Mo foil

On a Au foil, which should be inert to S, only an initial, limited formation of sulfidized Ti was observed. With further deposition there was no development of a sulfide layer. The initial deposition is possibly favored by surface active sites or impurities. In the same experiment, also a Ta foil was used as substrate beside Au. In Fig. 4.5 the difference can be clearly appreciated. The Ti 2p intensity grows as long as the $TiCl_4$ and TBDS flux continues. In this case also the substrate sulfidizes: the Ta 4f peak dramatically changes its shape, showing a component at higher BE

corresponding to the sulfide. In comparison with Au 4f, the Ta 4f peak is largely attenuated. This can only be partly attributed to the intermixing of Ta with S. The decrease is a clear indication of the formation of the TiS_2 overlayer. Indeed, after prolonged deposition times only the Ti and S signals remain present.

The surprising difference between Mo and Ta as a substrate may be explained by arguments given by Rodriguez in his studies on H_2S and S_2 adsorption on oxide catalysts [190, 191]. He found that the interaction of S with the substrate was weaker with compounds having a large band gap, such as Al_2O_3 compared to e.g. Cr_2O_3. Perturbation theory indicates that the half-filled $2\pi_g$ orbitals in S_2 are excellent electron acceptors. A larger band gap generally implies a lower position of the valence band maximum E_{TVB}, and a smaller heat of adsorption Q, according to refs. [192, 193]:

$$Q \propto (E_{TVB} - E_{2\pi}) \qquad \textit{(Eq. 4.2).}$$

The heat of adsorption at a given temperature determines the surface concentration of a species. The high activity of the precursors on or above the surface is the necessary condition to the fast growth of a thin film. The activity is a measure of both reactivity and abundance of the species. Therefore in CBE the thin film growth depends dramatically on the heat of adsorption of the precursors on the substrate used. The reaction of both metal substrates Mo and Ta with S_2 has to be fast, with formation of a layer of MoS_2 and TaS_2, respectively. Being MoS_2 a semiconductor and TaS_2 a metal, by applying Rodriguez's argumentation to our case, it can be supposed that the two substrates behave differently. Once the sulfide has formed, in the case of the Mo substrate S_2 does not remain adsorbed strongly enough, and also $TiCl_4$ desorbs not finding any reactive sites. The same assessment can also explain the low reactivity on the SiO_2 and Al_2O_3 substrates, which are expected to weakly adsorb S_2.

Also using stainless steel V4 TiS_2 could be formed in thick layers. But in this case a Cr signal remains always present (Fig. 4.6). The sulfidation behavior of Cr and its alloys is important in coal and oil industries and has been well investigated. It has been found that sulfide scales grow by an outward diffusion of Cr atoms through vacant metal sites [194, 195].

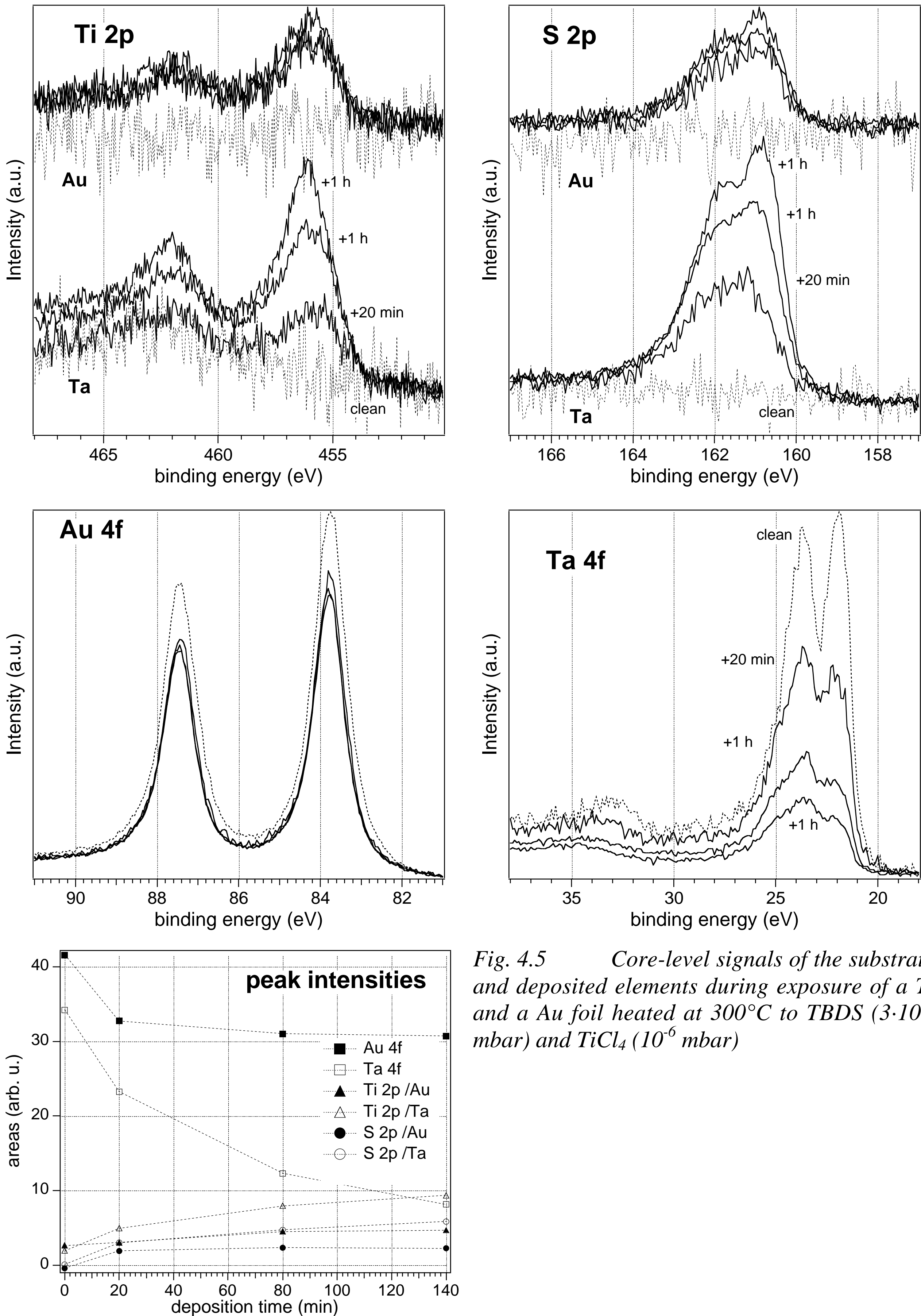

Fig. 4.5 Core-level signals of the substrate and deposited elements during exposure of a Ti and a Au foil heated at 300°C to TBDS ($3 \cdot 10^{-5}$ mbar) and $TiCl_4$ (10^{-6} mbar)

Ti itself could be used as substrate. A Ti layer was deposited on both Au and Ta (Fig. 4.7). Then TBDS only was exposed for 80 min. It can be clearly seen that the Ti 2p signal shifts to the typical position of the sulfide, but with a residual asymmetry, which indicates that even in this thin layer Ti did not react completely with S. From the peak width it is evident that the reaction proceeds better on the Ta substrate than on Au. This may be interpreted as a catalytic role of Ta. In catalysis it is well known that a second metal may promote the activity of a substrate. With respect to sulfidation, it has been found that some adsorbed transition metals are able to promote the formation of MoS_x [191, 196, 197] if S_2 was deposited on Mo(110). The promotion was explained as an increased electron density on Mo, which becomes available for the interaction with S_2 as an electron acceptor [190]. Therefore in the case of TiS_2 formation one may argue that Ta is able to increase the electron density of Ti, or at least not to decrease it, as is instead expected for the case of Au, which by itself tends to show a repulsion for S [198].

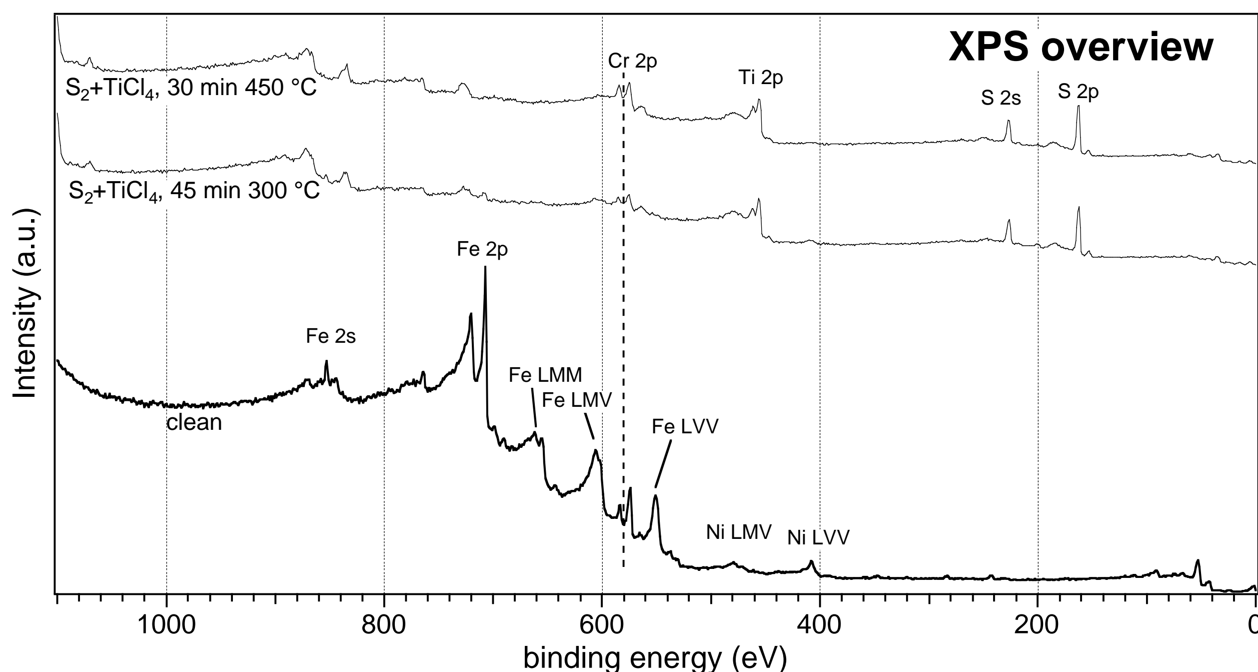

Fig. 4.6 XPS overview spectra for the deposition of S_2 and $TiCl_4$ on a stainless steel plate

On Ti foils or thicker Ti layers the sulfidation runs better if TBDS is co-evaporated with $TiCl_4$. This is an evidence that in these conditions Ti is not able to diffuse fast enough from the substrate to the surface reaction layer. Thus, for the growth of thicker films TiS_2 is deposited by both precursors, while the substrate takes an important part only to the nucleation steps.

Given the high sticking coefficient of metallic Ti on most substrates, TiS_2 thin films could be grown on variable supports, after a close Ti layer was evaporated.

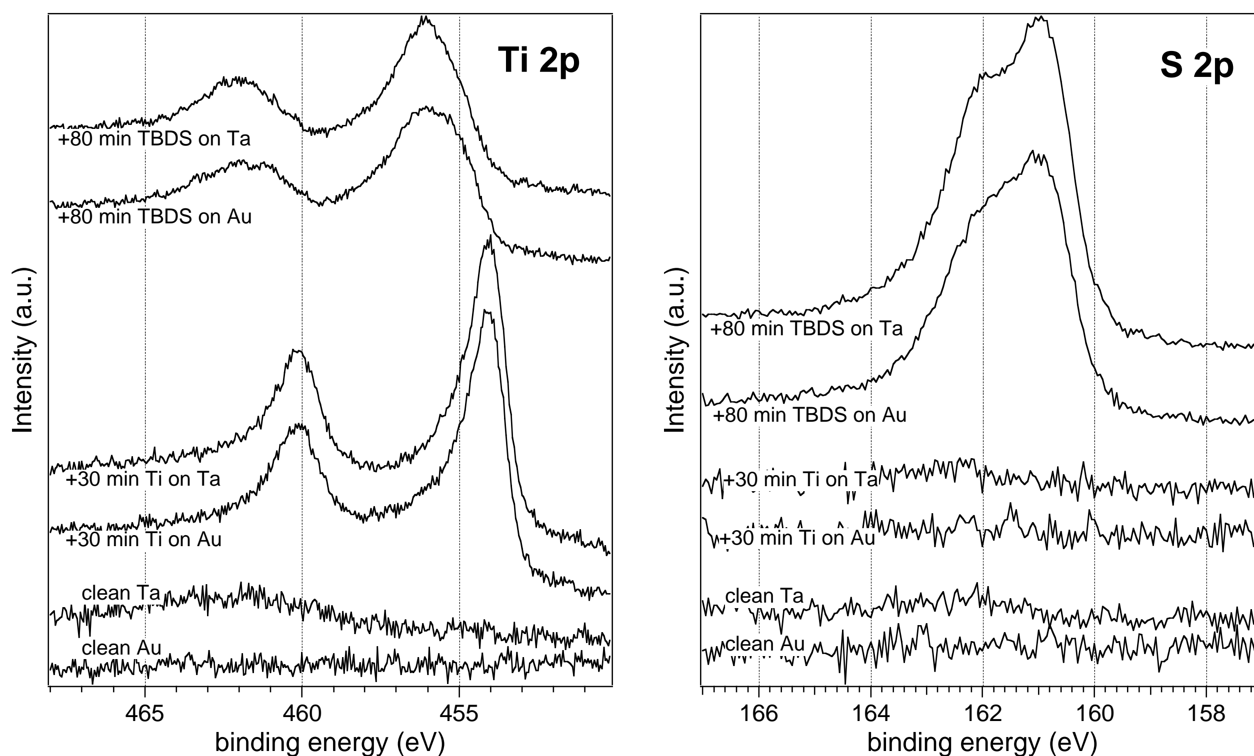

Fig. 4.7 Ti 2p and S 2p core levels obtained after the evaporation of Ti and subsequent TBDS exposure onto a Ta and a Au foil

4.3.3 Pressure and temperature

The phase diagram reported in Fig. 4.2 is relatively simple on the S-rich side. One would expect to prepare TiS_2 above 632°C, with a large S excess. This would correspond to an equilibrium between TiS_2 and nearly pure S liquid phase that, given the vacuum conditions, should be present only in minor amounts. However, these conditions could not be reached in the used growth chamber. The high local S pressure to have a liquid S phase at that temperature implies a too high partial S pressure in the chamber, which would burn the hot filaments. Therefore lower temperatures were used at the risk of TiS_3 formation.

In choosing the evaporation rates there is a tradeoff between growth rate and equipment safety. If, roughly, more product is obtained by increasing the precursors' partial pressure, the reactive species may create corrosion problems and decompose the oil in ball bearings and roughing pumps. However, within the limits of pressure of CBE, rates were considered to be low enough and modifications in order to provide a proper purging of the preparation chamber were not done. Once the substrate reached the deposition temperature, the evaporation rates were regulated by the stationary partial pressure obtained in the chamber. $TiCl_4$ was dosed by opening the corresponding fine dosing valve until the total pressure settled at 10^{-6} mbar. Given the tendency to form understoichiometric $Ti_{1+x}S_2$ compounds, a large excess of TBDS was used and the corresponding valve was opened up to a total pressure of $3 \cdot 10^{-5}$ mbar. The pressures were not further optimized,

but the tendency to deposit Ti in excess with lower TBDS/$TiCl_4$ ratios could be noted. With a total pressure of $3\cdot10^{-5}$ mbar the pressure inside the molecular beam may be much higher, even above the CBE limit. The beam was proven by well-focused shadows formed on the substrate, if a clip was masking the sample at a distance of a few mm from the surface.

In Fig. 4.8 an experiment series is reported, where the deposition on a Ta substrate was performed for periods of 20 min. The temperature was either set at fixed values or swept from 200 to 500°C. With a fixed temperature of 200°C only a small amount of Ti and S was deposited. The DOS near the Fermi level is dramatically reduced, as indicated by the He I valence band spectrum. The main broad peak in the range from 7 to 1 eV can already be attributed to S 3p states. The 1.4 eV increase of the work function indicates the formation of a surface phase with the properties of a sulfide. The sulfur deposition is evident from the S 2p core-level emission, and the Ti 2p signal indicates the Ti deposition. However, a new doublet at higher BE in the Ta 4f substrate spectrum strongly suggests also a partial Ta sulfidation. After the initial experiment the substrate temperature was varied in a ramp between 300 and 200°C. More details appeared in the S 3p region, while between 1 eV and the Fermi edge the EDC increases indicating the appearance of the Ti 3d emission of TiS_2. Almost an identical valence band was obtained by keeping the temperature at 300°C. The Ti and S signal clearly increased and the Ta 4f signal clearly decreases. This proves that the growth was much faster at this temperature, and is strongly inhibited a few tens of degrees below. With the next temperature ramp the valence band exhibited nearly no change, while at 400°C many spectral details are lost, and the Ti 3d conduction band states show a higher occupation with electrons. This is a clear sign that the S pressure above the sample is too low at this temperature and desorption is too fast to keep the sample stoichiometric. Nevertheless the sulfidated Ta component dominates the Ta 4f spectrum, suggesting that at this temperature range Ta reacts more rapidly with S. The valence band obtained after the temperature ramp ending at 300° is similar to that fixed at 300°C. This proves that at temperatures slightly higher than or equal to 300°C the growth is fast enough to build a homogeneous layer. The Ti 2p line confirms with its broadening the increased Ti 3d population at 400°C. Also in this case the best spectral shape is obtained for a substrate temperature of 300°C. The S 2p core levels do not show pronounced differences but reflect the shift of the Fermi level. The intensities of the core levels above 300°C show only a small increase, as the film thickness is already larger than the signal depth. At 500°C all features in the He I spectra of the S 3p group are lost. Probably at this temperature S evaporates from the film which becomes thinner. Additionally Cl may etch Ti, with a reaction of the kind

$$TiS_2 + 3TiCl_4 \rightarrow 4TiCl_3\uparrow + S_2 \qquad \textit{(Eq. 4.3)},$$

A thinner TiS_2 layer may explain the slight increase of the Ta 4f peak after the 500°C deposition. However, it may also be possible that at this temperature Ta diffuses into the Ti sulfide layer. Afterwards, depositions at 400 and 300°C give spectra identical to those taken during the series at increasing temperature, while the intensity of the substrate Ta 4f signal decreases until it completely disappears. The experiment clearly indicates that at the temperature of 300°C the given evaporation rates were adequate to obtain a satisfactory growth rate and well-resolved and narrow XPS and UPS emissions. This proves that a homogeneous chemical phase of adequate stoichiometry was deposited. Using Eq. 4.1 and the maximum value of E_{CB} of 0.3 eV a stoichiometry better than $Ti_{1.2}S_2$ can be estimated. Indeed, even on single crystals spectra indicating larger deviation of TiS_2 stoichiometry are possible (see next chapter). Spectra obtained after 5 days demonstrate the stability of the thin films in UHV.

No contamination of C, O or Cl were detected exceeding the sensitivity of core-level photoelectron spectroscopy (<0.2%). The measured He I and II valence band structures match calculations of integrated density of states and closely resemble XPS valence bands reported in literature [84, 199]. Evidently a randomly distributed orientation of the crystallites has been obtained during deposition.

Similar PES signals were obtained for distinct samples deposited at once at 300, 400 or 500°C on a Ti plate. Although less stoichiometric, samples prepared at higher temperature were more stable if subject to a subsequent annealing. This may indicate a larger crystal size in the films prepared at high temperature. Samples exhibiting small-sized crystals offer a larger amount of crystal edges, where S is more loosely bond. A valence spectrum similar to those obtained at 300°C could be measured after prolonged deposition at 200°C on a Ti plate (Fig. 4.9). The Ti core level shows two components indicating a very thin TiS_2 layer. Subsequent annealing at 200°C evidently leads to S evaporation from the layer and largely non-stoichiometric $Ti_{1+x}S_2$ is formed. If the deposition is done at 400°C the sample is again decomposed during annealing sequences at the deposition temperature, but remains stable below. This may be due to thicker films. In any case annealing at the deposition temperature has a detrimental effect. Thus for routine preparation of TiS_2 thin films only the $TiCl_4$ valve was soon shut at the end of the deposition time. The temperature was then slowly decreased from 300 to 250°C, corresponding to a typical time of 5 min, before also the TBDS source was closed.

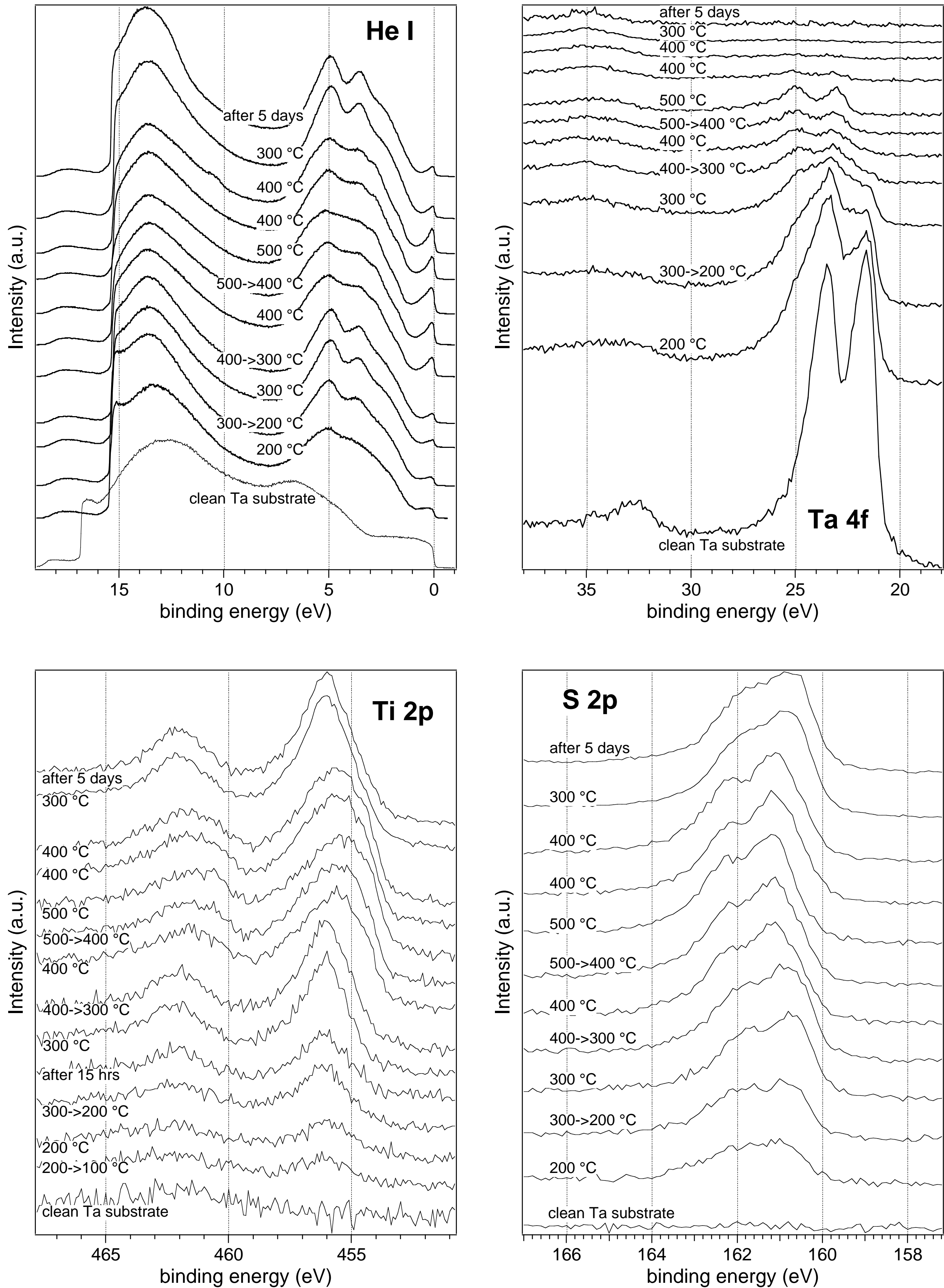

Fig. 4.8 UPS He I valence band, and Ta 4f , Ti 2p, S 2p XPS core levels obtained by the simultaneous evaporation of $TiCl_4$ (10^{-6} mbar) and TBDS ($3 \cdot 10^{-5}$ mbar) onto a Ta foil kept at different temperatures. Each deposition lasted 20 minutes

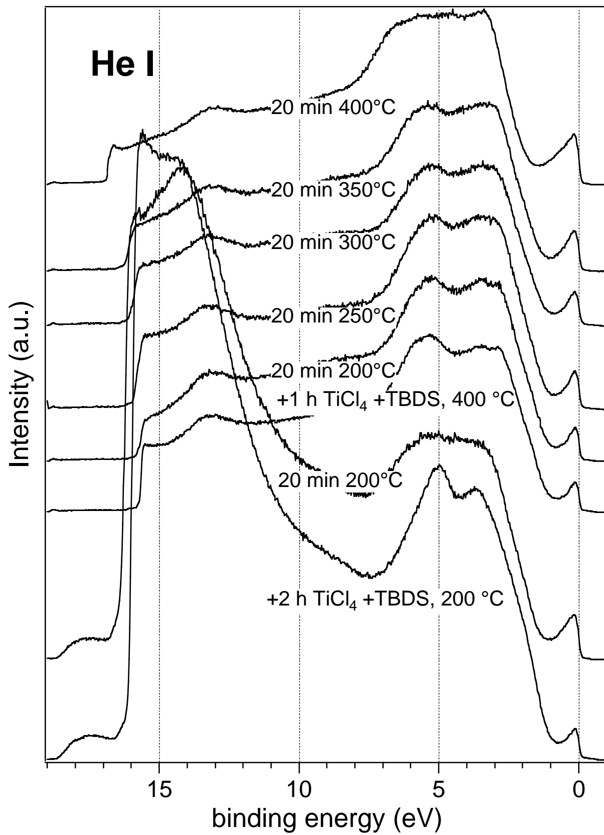

Fig. 4.9 UPS He I valence band, and Ti 2p, S 2p XPS core level emissions after the simultaneous evaporation of $TiCl_4$ (10^{-6} mbar) and TBDS ($3{\cdot}10^{-5}$ mbar) onto a Ti foil followed by heating periods

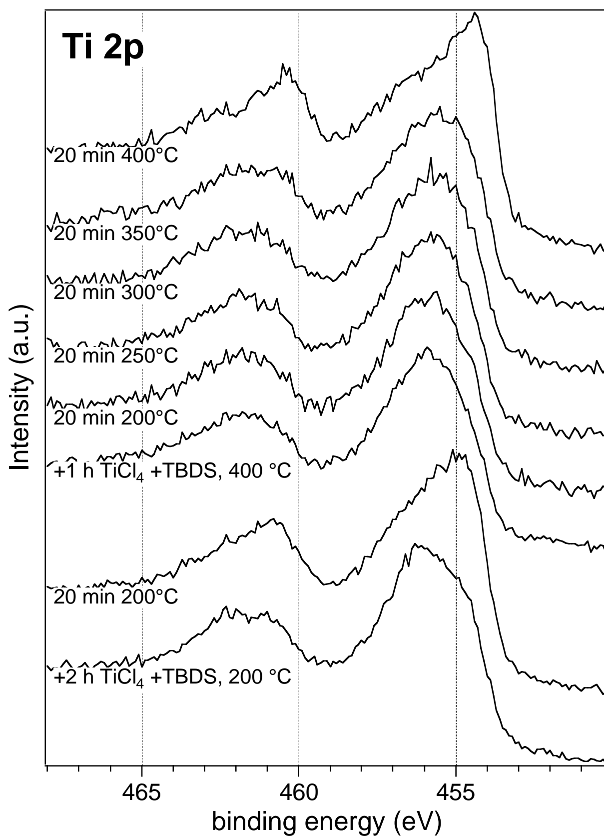

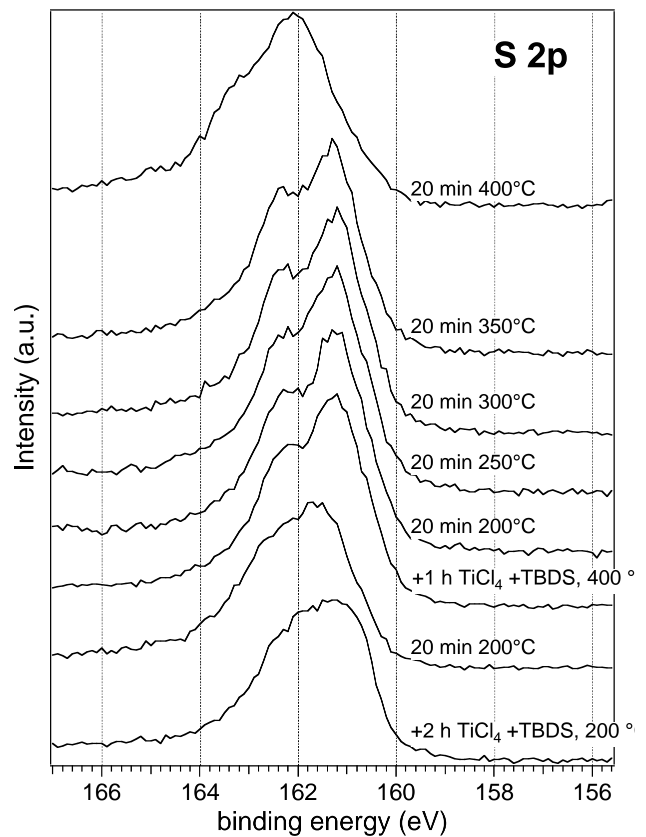

Chang and Schleich prepared TiS_2 by MOCVD using the reaction of $TiCl_4$ with TBDS, tert-butyl sulfide $(CH_3)_3C\text{-}S\text{-}C(CH_3)_3$, and HMDST [150]. In all three cases they obtained $Ti_{1+x}S_2$

deposition on several substrates, including stainless steel, Ti, and glass at temperatures ranging from 200 to 500°C. The only difference they noticed between the monosulfides and TBDS was the formation of TiS_3 from TBDS below 400°C. In particular, at 260°C only TiS_3 was obtained. The formation of TiS_3 can be definitely ruled out in the present CBE preparation. TiS_3 corresponds to the formal oxidation states $Ti^{4+}(S_2)^{2-}S^{2-}$ with two inequivalent S. S 2p core-level spectra reported in the literature clearly show two components with a BE difference at 1.4 eV to each other [200]. As Chang and Schleich commented in their work they could obtain TiS_3 by preventing the decomposition reaction

$$2TiS_3 \rightarrow 2TiS_2 + S_2 \qquad (Eq.\ 4.4)$$

with an increased sulfur pressure, which at 260°C was high enough to displace the equilibrium to the left. For the partial vapor pressure of sulfur above TiS_3 they reported the empirical relationship from ref. [201]:

$$\log P_{(mmHg)} = 10.42 - 6850/T \qquad (Eq.\ 4.5).$$

For 573 K one obtains a pressure of 30 mTorr, corresponding to about $4 \cdot 10^{-2}$ mbar, a pressure unlikely in the beam used for CBE. Therefore the equilibrium is displaced toward the decomposition of TiS_3 in TiS_2, and TiS_2 is obtained in UHV deposition as requested here.

4.4 The reaction mechanism

Schleich obtained for the reaction between $TiCl_4$ and TBDS in the liquid phase [150]

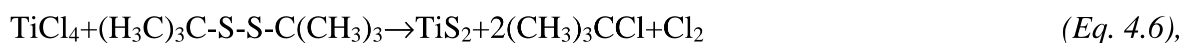

$$TiCl_4+(H_3C)_3C\text{-}S\text{-}S\text{-}C(CH_3)_3 \rightarrow TiS_2+2(CH_3)_3CCl+Cl_2 \qquad (Eq.\ 4.6),$$

but the reaction in MOCVD process was expected to be different. Bock and Mohmand [202] found that the pyrolysis of TBDS at 377°C proceeds according to the reaction:

$$(H_3C)_3C\text{-}S\text{-}S\text{-}C(CH_3)_3 \rightarrow 2[(H_3C)_2C{=}CH_2]+H_2S+1/8S_8 \qquad (Eq.\ 4.7).$$

The corresponding monosulfide decomposes at a 200°C higher temperature without production of S_8. This was explained with the higher energy of the S-C bond compared to the S-S bond ($\Delta H_b \approx 272$ kJ/mol vs. 226 kJ/mol). The mechanism proposed for TBDS decomposition involves the formation of radical species:

$$(H_3C)_3C\text{-}S\text{-}S\text{-}C(CH_3)_3 \rightarrow 2(H_3C)_3C\text{-}S^{\bullet} \qquad (Eq.\ 4.8),$$

$$(H_3C)_3C\text{-}S^{\bullet} +(H_3C)_3C\text{-}S\text{-}S\text{-}C(CH_3) \rightarrow (H_3C)_3C\text{-}SH+(H_3C)_3C\text{-}S\text{-}S\text{-}C(CH_3)_2C^{\bullet}H_2 \qquad (Eq.\ 4.9),$$

$$(H_3C)_3C\text{-}S\text{-}S\text{-}C(CH_3)_2C^{\bullet}H_2 \rightarrow (H_3C)_3C\text{-}S^{\bullet}+1/8S_8+(H_3C)_2C{=}CH_2 \qquad (Eq.\ 4.10),$$

$$(H_3C)_3C\text{-}SH \rightarrow (H_3C)_2C{=}CH_2+H_2S \qquad (Eq.\ 4.11).$$

This mechanism has been confirmed by mass-spectrometry analysis, but the decomposition was found already at 300°C [189]. With tert-butylsulfide the species $(H_3C)_3C\text{-}S\text{-}C(CH_3)_2C^{\bullet}H_2$ would

form in Eq. 4.9, whose decomposition will not produce $1/8S_8$. The nature of the $1/8S_8$ species has not been discussed in detail, but it is likely that under the reaction conditions S_2 and similar reactive S species are present. The formation of elemental sulfur appears to be the reason why even at higher temperatures TBDS behaves more like S_2 than TBS or HMDST. Indeed, also S_2 is a radical species. It is not only more reactive than H_2S but also has a higher heat of adsorption for the same substrate. According to Rodriguez *et al.* [203] H_2S adsorbs essentially as electron donor with its lone pairs. HS, S_2 and S have partially occupied orbitals at similar energies (10 to 11 eV below the vacuum) which are excellently situated for electron acceptor interactions. A metallic substrate with a Fermi level about 5 eV below vacuum (as given by the typical work function) acts as electron donor to S radical species. The same levels are already fully occupied if the species is not a S radical, therefore it will not be able to adsorb with the same mechanism. Therefore already from the point of view of adsorption energy, it is possible to foresee a much higher surface S concentration during deposition if radical species are involved.

The Ti-Cl bond is quite strong (389 kJ/mol), and in the gas phase $TiCl_4$ is stable up to temperatures of 1000°C [204]. In practical cases it is known that without external excitation sources e.g. such as excimer lasers temperatures of 1200°C are necessary to obtain the deposition of Ti from $TiCl_4$ [205]. Thus, even at MOCVD pressures a gas phase decomposition reaction cannot be supposed in the temperature regimes typically used for the reaction with TBDS. Lee used a Ti plate heated to 900°C to reduce $TiCl_4$ to $TiCl_n$ (n=1, 2, 3). From these chlorides metallic Ti could be deposited onto different substrates at 550-650°C [205]. This proves that the most difficult step is the reduction of $TiCl_4$, while lower chlorides are easier to decompose. In the present synthesis at 300°C a direct reaction of $TiCl_4$ with the surface sulfur species must occur. Winter and co-workers succeeded to prepare several $TiCl_4$ adducts with organosulfur compounds that are stable at room temperature [206]. Such compounds, where each Ti is coordinated by two further S, were demonstrated to be effective single-source precursors for the TiS_2 CVD synthesis, and are proposed as possible intermediates in the gas phase MOCVD reaction between $TiCl_4$ and organosulfides. With disulfides, and particularly with TBDS, no clear intermediate compound could be identified.

In order to shed light on the reaction channels, or at least on the secondary products obtained, a quadrupole mass spectrometer directly connected to the reaction chamber was used. Although data interpretation is complicated by reactions in the gas phase, the presence or absence of specific peaks could give some information.

The peak intensities reported in Fig. 4.10 refer to a TBDS beam directed into the chamber against a stainless steel plate. In order to distinguish between gas phase reactions and surface reactions mass spectra were taken as function of the substrate temperature, which was first

increased and then decreased again. The relatively small hysteresis of the peak intensities indicate that variations are directly related to the substrate temperature, and no possible side reactions developed with time in the gas phase or at the chamber wall. It may be questionable if all the surfaces that change temperature are of measured sample temperature. The heater filaments have indeed a temperature much higher than the sample and other parts close to it. Nevertheless, the cross section of the sample surface should be much higher than the hotter surfaces, as the beam was directed to it. The variations of peak intensities in the mass spectrum in dependence of temperature agree in part with those reported in ref. [189]. The decrease of the TBDS molecular peak (*m/z* 178) does not start at 300°C, but already quite steeply at 100°C, and the slope decreases above 300°C. This may suggest that the decomposition already starts at lower temperatures because catalyzed by the substrate. For higher temperatures the desorption rate increases, which affects the decomposition rate. Due to this early onset of decomposition the maximum amount of the intermediate $(H_3C)_3C\text{-}S\text{-}H$ (*m/z* 90) is not at 400°C, but below 350°C. The decomposition products of this intermediate, $(H_3C)_2C{=}CH_2$ (*m/z* 56) and H_2S (*m/z* 34) are given by ref. [189] as increasing with the temperature. In this case it can be seen that at 400°C the former reaches a plateau, and the latter has a maximum. Therefore, the substrate evidently promotes a further decomposition of these two species. The increase of molecular hydrogen H_2 (*m/z* 2) may suggest the reaction of S with the metallic substrate M:

$$(H_3C)_3C\text{-}SH + M \rightarrow (H_3C)_2C{=}CH_2 + H_2 + MS \qquad \textit{(Eq. 4.12).}$$

The S_2 (*m/z* 64) peak remains unchanged, while the S_8 (*m/z* 256) was beyond the spectrometer range.

The mass spectra of $TiCl_4$ alone did not show clear changes up to temperatures of 350°C (not shown).

By simultaneously evaporating $TiCl_4$ and TBDS below 300°C, following changes were observed according to the spectra of single precursors: no variation of the $TiCl_4$ peaks, a decrease of the unreacted TBDS. No trace was found, at any temperature, of a peak at *m/z* 92, which would correspond to the liquid-phase reaction product $(CH_3)_3CCl$. Relative to the spectra with TBDS alone, the peak *m/z* 90 as well as *m/z* 34 nearly vanished at RT. This suggests that even at RT S-containing fragments of TBDS do not desorb, but interact with $TiCl_4$. Among the alkyl fragments those increase which, like $(H_3C)_2C{=}CH_2$, are produced by the decomposition of these intermediately formed species. The trends observed already at RT are confirmed by heating the substrate: while the TBDS molecular peak shows its usual decrease, the S products all remain at very low levels, and *m/z* 56 has a clearer increase. Also the H_2 level remains low, likely because of

the reaction with Cl to produce HCl in strong progression with temperature. The increasing TBDS decomposition above 300°C affects even the $TiCl_4$ peak.

During TiS_2 deposition typically a decrease of HCl and an increase of TBDS were observed. This suggests that TiS_2 as substrate has a poorer catalytic activity than the metal, and implies that the deposition rate should decrease with film thickness.

The results given by the mass spectra suggest a reaction between the precursors which are favored by their good adsorption on the substrate and takes place without a preliminary pyrolysis. As evidently radical S species must be able to attack the Ti center, the Ti-Cl bond cleavage may be assisted by co-adsorbed H. Starting from 300°C, the faster TBDS pyrolysis accelerates the TiS_2 formation to the rates required during the deposition experiment.

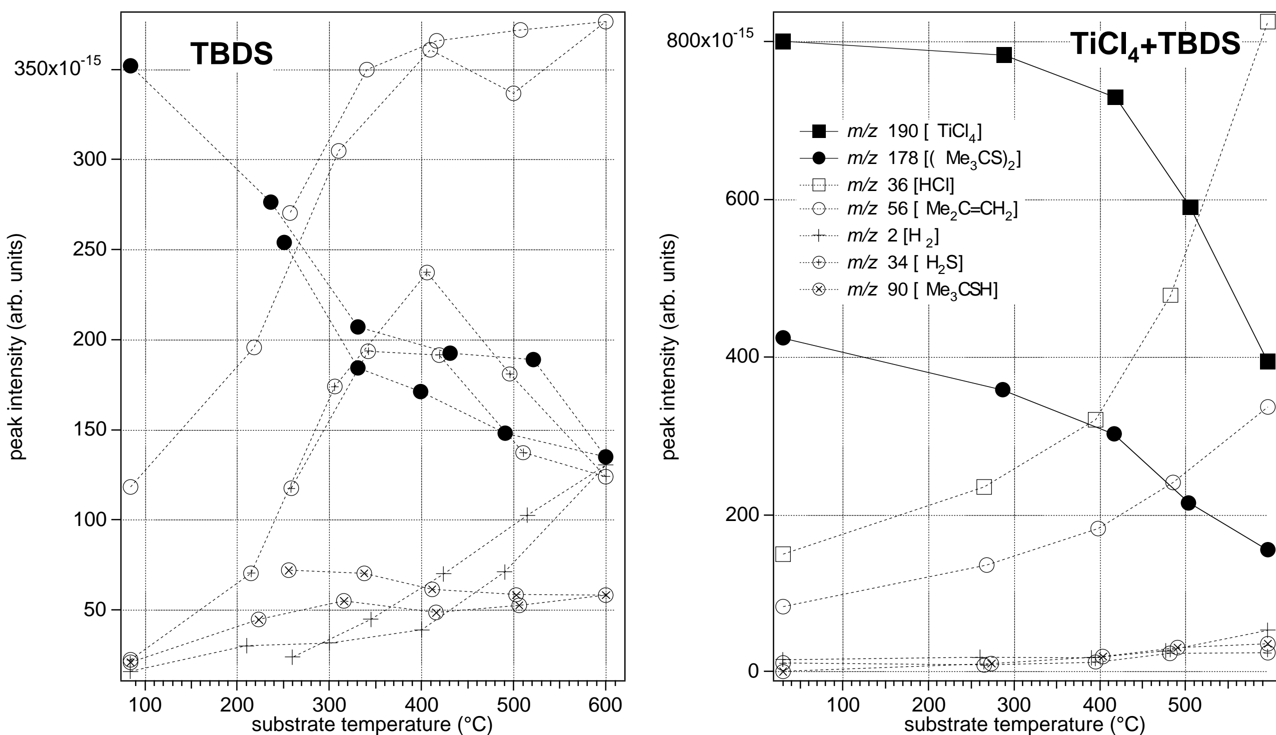

Fig. 4.10 Temperature dependence of mass spectra (ion peak intensities) corresponding to TBDS ($1.7 \cdot 10^{-5}$ mbar) and its gaseous decomposition products after adsorption on a stainless steel plate in UHV and after adding $TiCl_4$ up to a total pressure of $3.8 \cdot 10^{-5}$ mbar

4.5 Ex-situ characterizations

Leaving TiS_2 in vacuum prevents not only adsorbate formation, but also surface reactions. According to ref. [207] the sample surface hydrolyzes in contact with atmospheric moisture, and forms TiO_2 (anatase):

$$TiS_2 + H_2O \rightarrow TiO_2 + H_2S \qquad \textit{(Eq. 4.13).}$$

This was clearly confirmed with the thin films produced by CBE. In Fig. 4.11 core-level spectra of a TiS_2 film are shown after storing it 20 days at air. The Ti 2p line indicates the coexistence of two

components, one at the same BE as TiS_2, the other at the BE of TiO_2 [138]. The formation of TiO_2 is also indicated by the O 1s signal, which however shows two components, probably due to the presence of adsorbed OH^-. But also a S 2p signal is still measurable indicating that a surface TiO_2 film is formed, which is a few monolayers thick.

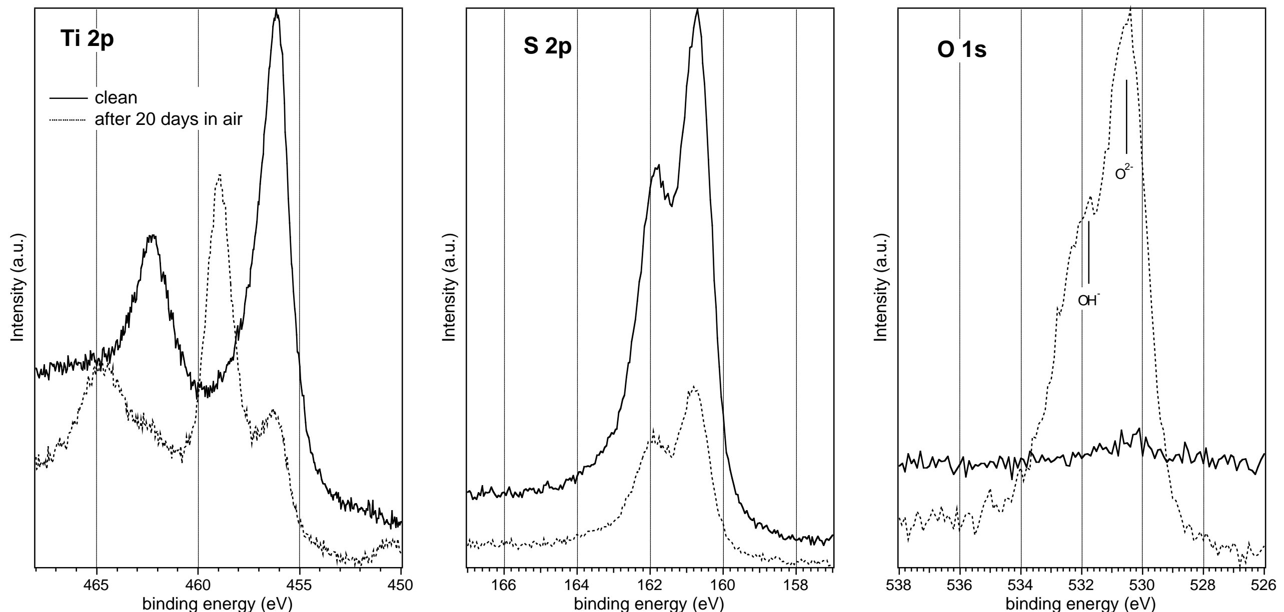

Fig. 4.11 The substrate core-level signals for a TiS_2 thin film before and after prolonged exposition to air

AFM

As the morphology of the substrate is important for thin film deposition, for the AFM measurement the sample was prepared on a polished Si (111) wafer, without further treatment. After degassing by heating to 450°C the substrate is terminated by an oxidized SiO_2 layer. To obtain TiS_2 growth on this substrate a metallic Ti layer was first deposited. Mounted close to the surface, a Ta foil was used to cover part of the sample during the Ti deposition, and was moved to another region during TiS_2 deposition. Four different regions are obtained: a) with no deposition, b) with only the Ti layer, c) exposed to the Ti and S precursors without the Ti layer, d) TiS_2 deposition with the usual process.

In regions a) and c) essentially the same flat surface was observed, with height variations in the order of a few Å, demonstrating again that no growth can be obtained under these conditions on SiO_2. In region b) the Ti layer could be seen with grains of a size of 50-100 nm, producing height irregularities of a few nm (Fig. 4.13). Any definite shape of the crystallites could not be recognized. A few holes were found, as the one in black in Fig. 4.13, probably resulting from areas which were covered by dust particles during the Ti evaporation. In region d) the roughness was larger, with irregularities of the order of 20 nm. A profile taken at the borderline between region c) and d) is

also shown in Fig. 4.14. A step could be easily identified, but it was not sharp enough to allow a precise determination of the film thickness. Although grains are larger than on pure Ti also on TiS_2 definite crystallites could not be identified. This may be attributed to the technique itself since the signal results from the convolution of the substrate with the scanning tip.

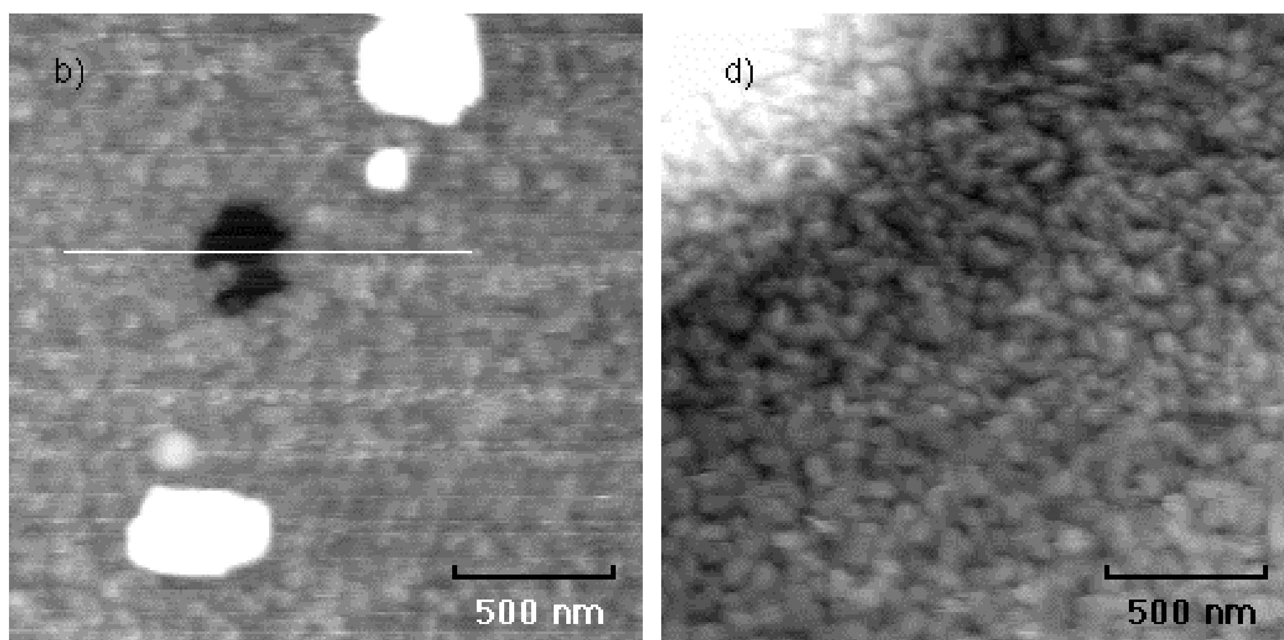

Fig. 4.12 AFM micrographs for the metallic Ti layer (b) and for the TiS_2 film (d)

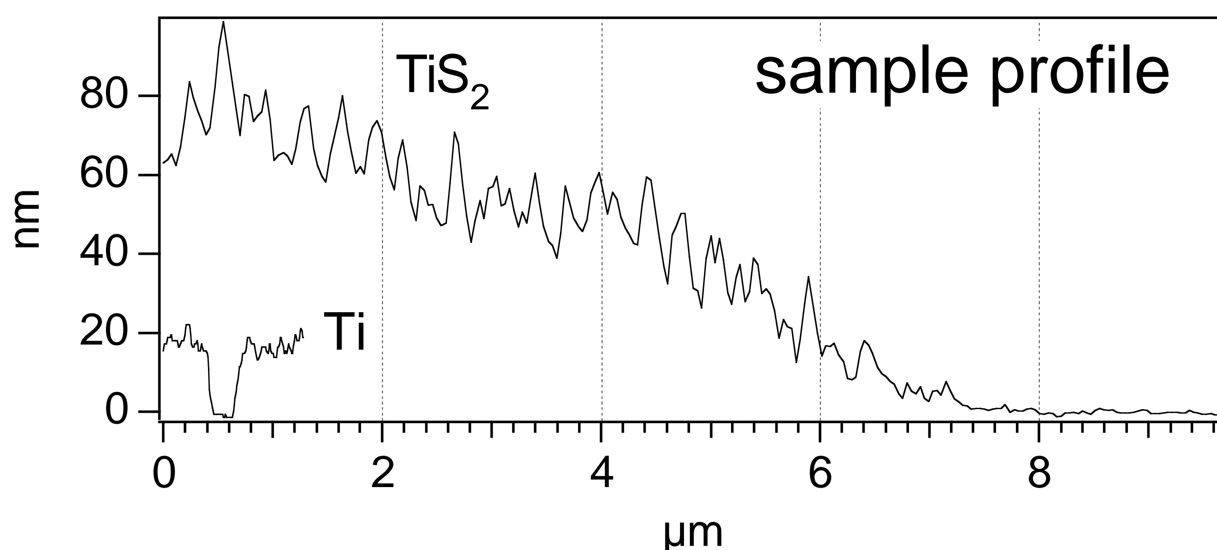

Fig. 4.13 Comparison between the topographic profiles as taken from the Ti layer (region b, corresponding to the line drawn in Fig. 4.12) and the TiS_2 film (region d, at the frontier with region c)

The white areas in region b) represented in Fig. 4.12 have a height of about 150 nm, and are probably Ti droplets, because in region a) dust particles always have a height of only a few nm. In region d) circular bubbles were found (part of one is on the top left corner of Fig. 4.13, right) of

similar height but of about 3 μm in diameter (Fig. 4.14). Evidently, the Ti droplets act as nucleation centers for the growth of TiS_2.

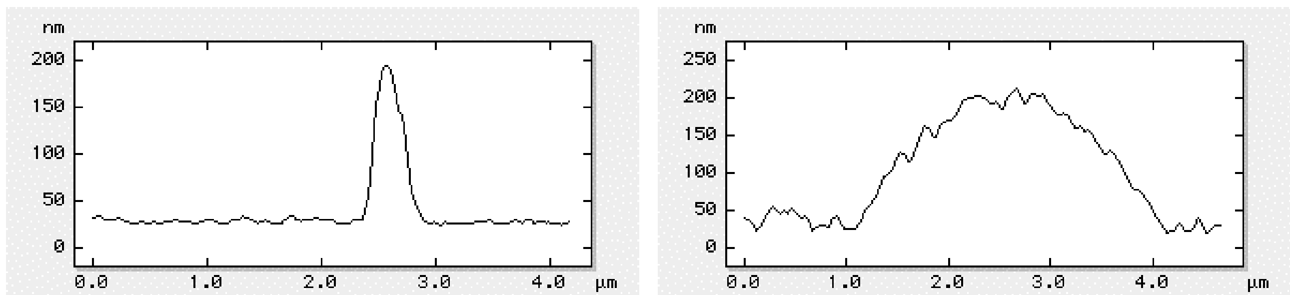

Fig. 4.14 Topographic profiles taken on particles present on the Ti layer (left) and on the TiS_2 film (right)

TEM

The crystalline nature of the sample is clearly shown by the images obtained by TEM (Fig. 4.15). A highly textured pattern strongly suggests the formation of platelets oriented perpendicularly to the substrate. Indeed a close examination of the darker bars reveals that they are typically grouped forming angles that resemble the top edges of nearly upright hexagons. The presence of ordered structures is visible in high-resolution images. Some spots can also be identified that suggest the presence of platelets also oriented parallel to the substrate (Fig. 4.15 bottom). Interference patterns are present not only in the zones corresponding to the bars, but are also found more diffuse in the background region. A Fourier transformation was done for several different regions in high-resolution pictures. The periodic distances found are represented in Fig. 4.16 Regions corresponding to the dark bars give periods scattered between 5.6 and 6.5 Å, with a maximum between 5.8 and 6.0 Å, which is somewhat higher than 5.7 Å for the (001) peak of hexagonal TiS_2. The background gives values which more closely agree to the reflexes (100) and (101). The precision and the scattering of these values does not allow the exact identification of the phases: however, given their related structures the non-stoichiometric phases exhibit distances which typically differ each other by less than 5%. With self-intercalation both **c** and **a** axes should expand [208]. Furthermore the most typical reflexes for cubic TiS_2, for TiS_3, TiO_2 and Ti could not be found. In the diffraction mode reflexes for distances of 1.5, 1.7 and 3.5 Å were found, which may be assigned to TiO_2 (anatase).

Thus the TEM results support the identification from the photoemission data that TiS_2 is formed during the CBE process.

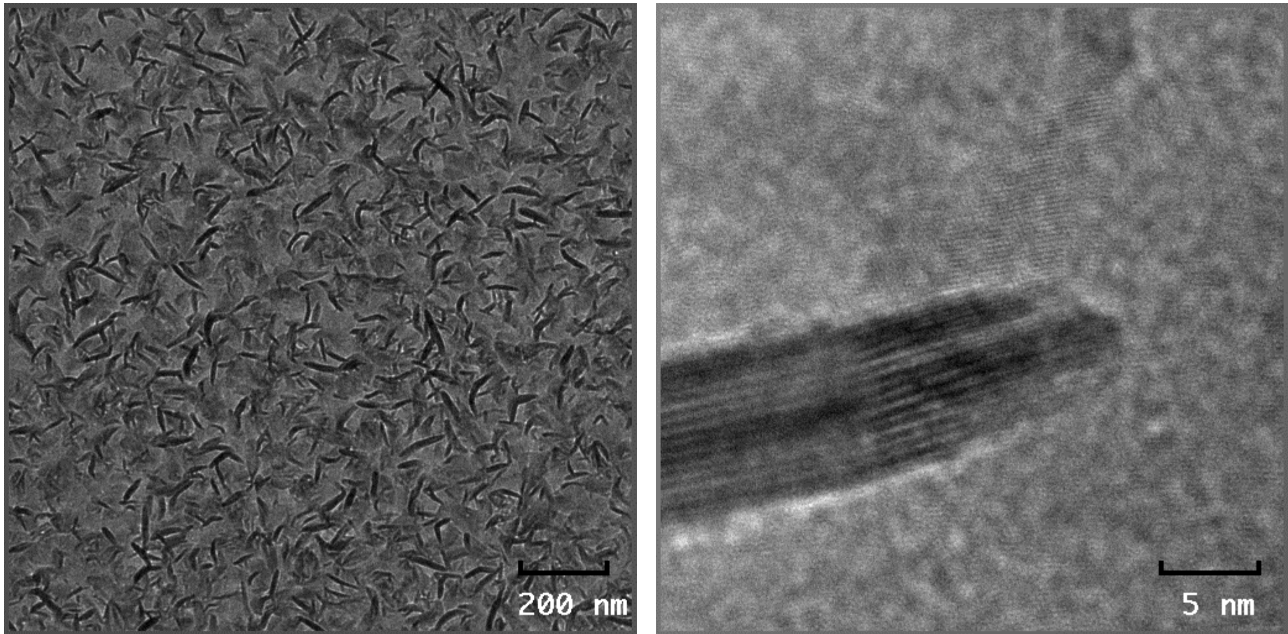

Fig. 4.15 TEM micrographs for TiS_2 thin films at magnifications of 9.6 k (above) and two different details at magnifications of 430 k (right)

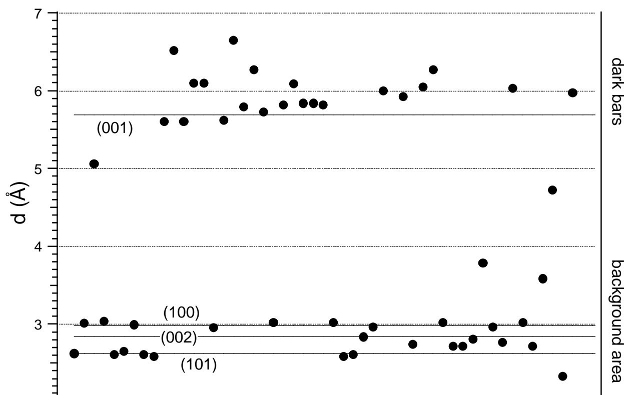

Fig. 4.16 Atomic distances calculated by FFT from several high-resolution TEM images, and a comparison with values of hexagonal TiS_2